Row–column visibility graph approach to two-dimensional landscapes*

Xiao Qin(肖 琴)[a], Pan Xue(潘 雪)[a], Li Xin-Li(李信利)[a)b)], Mutua Stephen[a)c)], Yang Hui-Jie(杨会杰)[a)†], Jiang Yan(蒋 艳)[a], Wang Jian-Yong(王建勇)[d)], and Zhang Qing-Jun(张庆军)[e)]

[a)] *Business School, University of Shanghai for Science and Technology, Shanghai* 200093, *China*
[b)] *Logistic School, Linyi University, Jinan* 276000, *China*
[c)] *Computer Science Department, Masinde Muliro University of Science and Technology, P.O. Box* 190-50100, *Kakamega, Kenya*
[d)] *Department of Physics, Xingtai College, Xingtai* 054001, *China*
[e)] *Analysis and Testing Center, Hebei Polytechnic University, Tangshan* 063009, *China*

(Received 27 December 2013; revised manuscript received 2 January 2014; published online 15 May 2014)

A new concept, called the row–column visibility graph, is proposed to map two-dimensional landscapes to complex networks. A cluster coverage is introduced to describe the extensive property of node clusters on a Euclidean lattice. Graphs mapped from fractals generated with the probability redistribution model behave scale-free. They have pattern-induced hierarchical organizations and comparatively much more extensive structures. The scale-free exponent has a negative correlation with the Hurst exponent, however, there is no deterministic relation between them. Graphs for fractals generated with the midpoint displacement model are exponential networks. When the Hurst exponent is large enough (e.g., $H > 0.5$), the degree distribution decays much more slowly, the average coverage becomes significant large, and the initially hierarchical structure at $H < 0.5$ is destroyed completely. Hence, the row–column visibility graph can be used to detect the pattern-related new characteristics of two-dimensional landscapes.

Keywords: row–column visibility graph, landscape, roughness

PACS: 89.75.Hc, 72.15.Rn, 05.50.+q, 05.45.Df **DOI:** 10.1088/1674-1056/23/7/078904

1. Introduction

Landscape is an essential concept in diverse research fields. About 50 years ago, protein molecules were demonstrated to fold into a three-dimensional native state reversibly, which leads to the view that these structures represent the global minimum of a rugged funnel-like energy landscape.[1,2] For an electron walking in a lattice, randomly distributed site energies may induce localization of its state, namely, it can be found only in a special region.[3–12] Patterns in the potential landscape determine the characteristics of its states, which can be used to understand marvelous properties of a large amount of materials. Anomalies of diffusion,[13–18] namely, the nonlinear temporal growth of the mean square displacement of Brownian particles, generally come from the heterogeneous potential,[19–24] parameter,[25–28] and/or viscosity[29–34] landscapes. Hence, how to describe quantitatively the landscapes is an essential problem.

The wavelet transform[35] is widely used to detect multifractal structures in landscapes.[36] The Hurst exponent can tell us in a global way the degree of roughness, while the multi-fractal spectrum has a nontrivial relation with the fine structures. However, the spectrum contains no explicit information on the localizations of the fine structures.

An alternative candidate method is the visibility graph,[37] a fundamental geometrical structure useful in many applications such as illumination and rendering, motion planning, pattern recognition, and sensor networks. It is conducted typically for a set of location points and obstacles in the Euclidean plane. The nodes and the edges represent the point locations and the visible links between them, respectively. Visibility between two nodes is defined when the straight link between them intersects no obstacle.

The structure of a landscape determines its visibility graph. Nontrivial characteristics of the visibility graph can be used to represent structural patterns for the landscape. By mapping a two-dimensional landscape to a visibility graph, the concepts in the complex network theory can be used to investigate detailed patterns of the landscape from micro- to macroscales. The degree and the clustering coefficient tell us the behaviors of each element. The motifs and the communities provide us with the structural characteristics of the local landscapes, while the backbone of the visibility graph captures the distribution behaviors of the extreme elements. In traditional series analysis methods, statistical quantities are obtained at different scales. The information on detailed structural pat-

*Project supported by the National Natural Science Foundation of China (Grant No. 10975099), the Program for Professor of Special Appointment (Eastern Scholar) at Shanghai Institutions of Higher Learning, China, the Innovation Program of Shanghai Municipal Education Commission, China (Grant No. 13YZ072), the Shanghai Leading Discipline Project, China (Grant No. XTKX2012), and the Innovation Fund Project for Graduate Students of Shanghai, China (Grant No. JWCXSL1302).

†Corresponding author. E-mail: hjyang@ustc.edu.cn

© 2014 Chinese Physical Society and IOP Publishing Ltd

terns are lost in the statistical procedure.

Very recently, the visibility graph was particularized to a one-dimensional (1D) version to map 1D landscapes (time series) to complex networks.[38] For a time series, one can regard data points as nodes and connect each node with all the nodes covered within its visible line. It is found that the 1D visibility graph inherits several properties of the corresponding time series, for example, the constructed graphs for periodic, random, and fractal series behave as regular, exponential, and scale-free, respectively. It is also powerful in detecting reliable values of the Hurst exponent for fractional Brownian motions[39,40] and in distinguishing chaos from noises.[41] It is used successfully to deal with real-world data, such as the currency exchange rate series[42] and heartbeat series.[43,44]

The complex network theory proves it is powerful in detecting topological characteristics for networked elements of complex systems. A natural idea is to investigate visibility graphs from the viewpoint of complex networks. However, when we address complicated landscapes with a large amount of point locations, a critical problem occurs that the corresponding visibility graphs are unacceptably dense. i.e, averagely, each node is linked with many other nodes. Our detailed calculations for the generated landscapes in this paper show that the average number of neighbors reaches several tens to several hundreds. When one tries to investigate the standard visibility graphs by means of the complex network theory, nontrivial behaviors in the topological structures are merged by the tightness of the graphs. Hence, a modification should be introduced to the standard visibility graph to balance the two competitive requirements, namely, capturing the structural information as complete as possible and keeping sparsity as possible.

In the present paper, a simplified version of the standard visibility graph is proposed to map two-dimensional landscapes to complex networks, called row–column visibility graph. We make a balance of the two competitive features by using the row and column visibility. It can be extended easily to address multi-dimensional landscapes and complicated landscapes without distinct definition of directions (coordinates). As examples, this new concept is used to measure quantitatively the structural patterns in model-generated two-dimensional (multi)-fractal landscapes.

2. Methods and materials

2.1. Row–column visibility graph for two-dimensional landscapes

A two-dimensional landscape on a regular lattice reads $\{z(i,j)|i=1,2,\ldots,M;\ j=1,2,\ldots,N\}$. One can regard the data points as nodes indexed with their addresses on the lattice (i,j). Each node is initially connected with its nearest neighbors, which results in a regular lattice.

Herein, we consider a simplified version of the standard visibility graph. For each node, we extract the column and the row in which it occupies and link it with all the nodes in the column and the row that are within its visible line. That is, the visibility between two points (i_a,j_a) and (i_b,j_b) refers to

$$\begin{cases} i_a = i_b, \\ j_a < j_c < j_b \text{ or } j_a > j_c > j_b, \\ z(i_a,j_c) < z(i_a,j_b) + [z(i_a,j_a) - z(i_a,j_b)]\,\frac{j_b - j_c}{j_b - j_a}, \end{cases} \tag{1}$$

or

$$\begin{cases} j_a = j_b, \\ i_a < i_c < i_b \text{ or } i_a > i_c > i_b, \\ z(i_c,j_a) < z(i_b,j_a) + [z(i_a,j_a) - z(i_b,j_a)]\,\frac{i_b - i_c}{i_b - i_a}. \end{cases} \tag{2}$$

The resulting graph is called a row–column visibility graph (RCVG).

As a note, we have also considered an extension of the RCVG, namely, for a node, besides the row and the column we also extract the diagonals it occupies and link it with all the nodes in the diagonals that are within its visible line. The constructed networks can also capture the nontrivial characteristics embedded in the generated landscapes, however, they cannot show us qualitatively new characteristics for the landscapes compared to that provided by the RCVGs.

2.2. Heterogeneity

Heterogeneity of a visibility graph, namely, the nontrivial deviation of its structure from the corresponding randomized networks, can represent the characteristics of the corresponding landscape. Several properties are used to detect the heterogeneities from micro- to macro-scale.

The degree of a node is the number of its nearest neighbors.[45] An exponential network means that the degree distribution function decays exponentially, $p(k) \sim \exp(-\alpha k)$. A large amount of real-world networks are scale-free, namely, the degree distribution obeys a right-skewed power law, $p(k) \sim k^{-\beta}$. In a scale-free network, there are some high-degree nodes acting as hubs, and there is no characteristic degree. The maximum-likelihood estimation is used to estimate the scaling exponent β,[46,47] i.e.,

$$\beta = 1 + \left[\sum_{k_{i,j}\geq k_{\min}} 1\right] \cdot \left[\sum_{k_{i,j}\geq k_{\min}} \ln\left(\frac{k_{i,j}}{k_{\min}}\right)\right]^{-1}, \tag{3}$$

where $k_{i,j}$ is the degree of node (i,j), and $k_{\min}$ is the smallest degree above which there exists a power-law relation. By setting the confidence level to 95%, the corresponding confidence intervals are obtained as shown in the results.

The clustering coefficient of node (i_0,j_0) is the probability of its neighbors' being connected with each other,[45] which reads

$$C(i_0,j_0) = \frac{2\Delta(i_0,j_0)}{k_{(i_0,j_0)} \times [k_{(i_0,j_0)} - 1]}, \tag{4}$$

where $\Delta(i_0, j_0)$ is the number of the edges between its neighbors.

By using the coordinates of the nodes in the two-dimensional lattice, one can calculate the Euclidean length for each edge in the constructed network, which may provide us with the extensive properties of the global network and each node. In the present paper, we define a new measure, called the cluster coverage, to measure quantitatively heterogeneity of spatially embedded networks. The average distance between each linked pair of nodes is

$$\langle D_{\text{link}} \rangle = \frac{\sum_{(i_0,j_0)=(1,1)}^{(M,N)} \sum_{(i,j)\in\Phi(i_0,j_0)} \left(|i-i_0|^2 + |j-j_0|^2\right)^{\frac{1}{2}}}{\sum_{(i_0,j_0)=(1,1)}^{(M,N)} k_{(i_0,j_0)}}, \quad (5)$$

where $\Phi(i_0, j_0)$ is the set of the nearest neighbors of node (i_0, j_0). The average distance between each linked pair of the neighbors of node (i_0, j_0) reads

$$D_{\text{cluster}}(i_0, j_0) = \frac{\sum_{(i_a,j_a)\neq(i_b,j_b)\in\Phi(i_0,j_0)} \left[(i_a - i_b)^2 + (j_a - j_b)^2\right]^{\frac{1}{2}} \cdot A\left[(i_a, j_a), (i_b, j_b)\right]}{\sum_{(i_a,j_a)\neq(i_b,j_b)\in\Phi(i_0,j_0)} A\left[(i_a, j_a), (i_b, j_b)\right]}, \quad (6)$$

where $\boldsymbol{A}$ is the adjacency matrix, namely, $A\left[(i_a, j_a), (i_b, j_b)\right] = 1$ if nodes (i_a, j_a) and (i_b, j_b) are connected, and it is 0 otherwise.

The definition of the cluster coverage reads

$$R_{\text{cluster}}(i_0, j_0) = \frac{D_{\text{cluster}}(i_0, j_0)}{\langle D_{\text{link}} \rangle}. \quad (7)$$

It tells us the relative volume of the cluster centered at node $(i_0,\ j_0)$ in the regular lattice. It describes the extensive property of the clusters.

A macro-scale property of a network is the modularity, namely, the network can be separated into some densely connected groups, while the groups are connected loosely with a few edges. Many real-world networks simultaneously have a high modularity and a high degree of clustering, and are scale-free. The coexistence of the three characteristics can be realized with the replica-based deterministic network model proposed by Barabasi *et al.*,[48] in which the groups are combined in a hierarchical manner. Such a hierarchical organization of the network imposes strict restrictions on the number and the degree of cohesiveness of the different groups, which can be measured by the following relation:[49]

$$C^*(k) \sim k^{-\gamma}, \quad (8)$$

where $C^*(k)$ is the average clustering coefficient over the nodes with degree k. This power law is found in many real-world networks.[50–53] If this relation stands, the exponent γ can be used as a quantitative description of the non-homogenous structure. The larger the exponent γ, the more significant the hierarchical organization.

2.3. Data

A large amount of two-dimensional landscapes have (multi-)fractal structures, which can be characterized by multi-fractal spectra.[35] A landscape can be decomposed into many subsets exhibiting different local Hurst exponents h. Each local Hurst exponent quantifies the local singular behavior and thus relates to the local scaling of the landscape. The multi-fractal spectrum is the occurring probabilities of all the subsets, called fractal dimensions for the subsets, denoted with $D(h)$. It is generally a bell-shaped curve. The strength of multi-fractal is measured by the width of $D(h)$, namely, $\Delta h = h_{\max} - h_{\min}$. The Hurst exponent of the landscape is the special local Hurst exponent at which $D(h)$ reaches its maximum value, i.e., $H = h_{\text{p}}\Big|_{\frac{\mathrm{d}D(h_{\text{p}})}{\mathrm{d}h}=0}$.

We consider two-dimensional deterministic multi-fractals generated by the probability re-distribution (PRD) model.[54] We can firstly construct a landscape on a 2×2 lattice, which reads

$$P_0 = \begin{bmatrix} p_{11} & p_{12} \\ p_{21} & p_{22} \end{bmatrix}, \quad (9)$$

where the elements are the occurring probabilities at the corresponding cells. The elements are non-negative and satisfy $p_{11} + p_{12} + p_{21} + p_{22} = 1$. It is used as a generator. A multi-fractal landscape on a two-dimensional regular lattice can be generated by iteratively re-distributing the probabilities. At each generation, each existing cell is divided into four sub-cells, and the probabilities are re-distributed into the sub-cells according to the generator, i.e.,

$$\begin{aligned} \boldsymbol{P}_1 &= \boldsymbol{P}_0, \\ \boldsymbol{P}_2 &= \boldsymbol{P}_1 \otimes \boldsymbol{P}_0, \\ &\cdots \\ \boldsymbol{P}_g &= \boldsymbol{P}_{g-1} \otimes \boldsymbol{P}_0, \end{aligned} \quad (10)$$

where $\otimes$ is the kronecker product.

We also consider two-dimensional random fractals constructed by the midpoint displacement algorithm (MDA).[55] The procedure starts from a rectangle as the seed. The heights of the four corners are assigned randomly. The vertical and horizonal lines that intersect at the center cut the seed into four

identical sub-rectangles. Five new-created corners appear, including the center and the midpoints of the four edges. In each edge, the two initial corners at the ends are called the parent of the midpoint. The height of the center is the mean of those of the four initial corners, while the heights of the four midpoints are the means of their parents. To obtain a fractal landscape with Hurst exponent value H, for each new corner we should add to its height a small error w sampled from an adjusted standard normal distribution function, which reads

$$F(w) \sim \frac{1}{\sqrt{2\pi}} \exp(-w^2) \cdot 2^{-gH} \cdot \sqrt{1-2^{2H-2}}. \qquad (11)$$

Iterate and subdivide each sub-rectangle into smaller ones until the expected number of corners is reached. The parameter g denotes the iteration number, namely, at the G-th generation, we have $g = G$. By this method, we can make the error proportional to the size of the sub-rectangle.

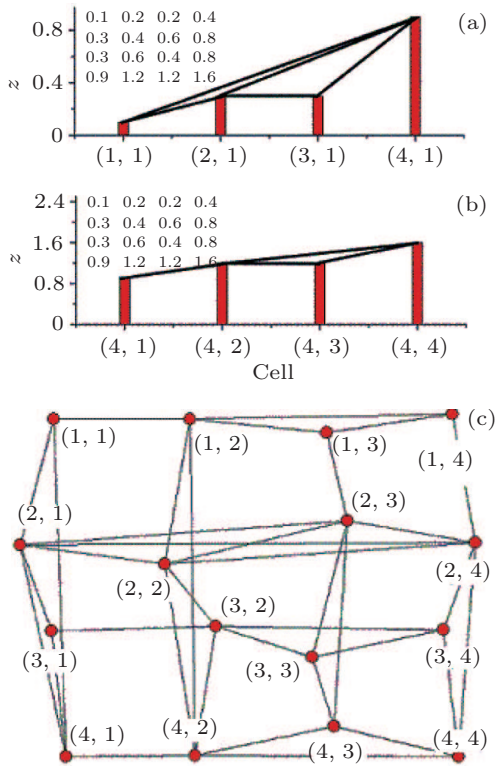


Fig. 1. (color online) Illustration of the procedures to construct a RCVG from a PRD fractal. The generator is $(p_{11},\ p_{12},\ p_{21},\ p_{22}) = (0.1,\ 0.2,\ 0.3,\ 0.4)$. After two generations, a 4×4 landscape is produced, as shown in panel (a): (a) connections between the nodes in the column in which node $(4,1)$ sits; (b) the connections between the nodes in the row in which node $(4,1)$ sits; (c) the resulting RCVG.

Figure 1 presents an illustration of the successive procedures from generating an PRD-fractal to constructing a RCVG. The generator is $(p_{11},\ p_{12},\ p_{21},\ p_{22}) = (0.1,\ 0.2,\ 0.3,\ 0.4)$. After two generations, the probability is distributed into 4×4 cells

$$10 \times \boldsymbol{P}_2 = \begin{bmatrix} 0.1 & 0.2 & 0.2 & 0.4 \\ 0.3 & 0.4 & 0.6 & 0.8 \\ 0.3 & 0.6 & 0.4 & 0.8 \\ 0.9 & 1.2 & 1.2 & 1.6 \end{bmatrix}. \qquad (12)$$

As an example, we choose the node $(4,1)$. Figures 1(a) and 1(b) show the connections between the nodes in the 1st column and in the 4th row (where the node sits in), respectively. Figure 1(c) gives the resulting RCVG.

We have carried out the calculations for different sizes, including 32×32, 64×64, 128×128 for PRD-fractals and 33×33, 65×65, 129×129 for MDA-fractals. The networks with sizes 64×64 for PRD-fractals and 65×65 for MDA-fractals have almost the same behaviors as those reported in this paper, though there is much significant fluctuation. Hence, we report the results for the PRD-fractals with size 128×128, and for MDA-fractals with size 129×129. The results for the MDA-fractals are the averages of 20 realizations.

3. Results

We consider firstly a random two-dimensional landscape whose elements are random real numbers normally distributed with mean 0, variance 1, and standard deviation 1. The degree distribution function obeys an exponential law, namely, $\sim \exp(-0.13k)$, as shown in Fig. 2(a). The $C^*(k)$ versus k obeys a power law, and the exponent is 0.84.

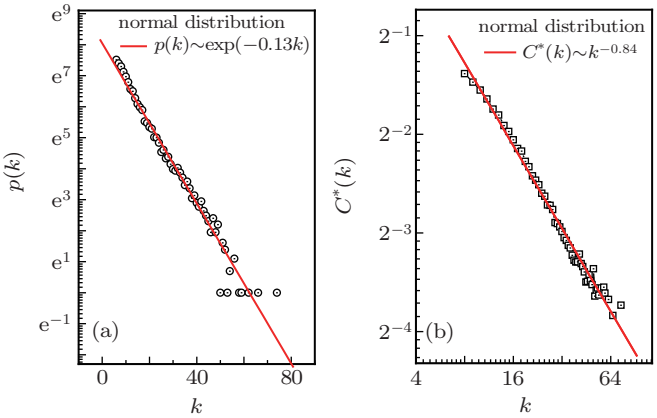


Fig. 2. (color online) RCVG for a random landscape with normally distributed elements. The size is 128×128: (a) the degree distribution function obeys an exponential law, the average degree is ~ 11; (b) the relation of $C^*(k)$ versus k obeys a power law.

We generate PRD-fractals with the generator $p_{11} = p_{12} = p_{21} = p$. The corresponding RCVGs behave scale-free, as shown in Fig. 3(a). With the increase of p, the scale-free exponent, β, increases and reaches the maximum value at $p = 0.27$, and then decreases rapidly (Fig. 3(b)). The landscapes are also shuffled by exchanging simultaneously the rows and the columns in a random way. Though the RCVGs for the shuffled landscapes are scale-free, β for the shuffled landscapes are significantly larger than that for the original PRD-fractals. Hence, the scale-free behaviors of the RCVDs are structure-related.

The $\langle C \rangle$ and $\langle R_{\text{cluster}} \rangle$ versus p are given in Fig. 4. The $\langle C \rangle$ for the PRD-fractals are smaller than for the corresponding shuffled landscapes, and the difference tends to be much

more significant when $p \to 0.25$. With the increase of p, $\langle R_{\text{cluster}} \rangle$ decreases and reaches the minima at $p = 0.27$, and then increases. When p deviates significantly from the special point $p = 0.25$, there exist distinguished differences between the original and the shuffled landscapes. The RCVGs for the original landscapes are comparatively much more extensive.

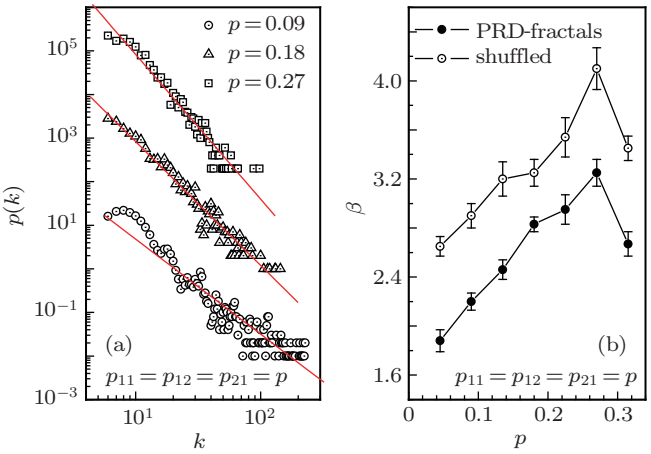


Fig. 3. (color online) Degree distributions of RCVGs for PRD-fractals. The generator is $(p_{11}, p_{12}, p_{21}, p_{22}) = (p, p, p, 1-3p)$. (a) The degree distribution functions obey the power law, the curves are vertically shifted for visualization convenience. The average degrees for the cases of $p = 0.09, 0.18, 0.27$ are $\sim 12, 10, 9$, respectively. (b) The β for the shuffled landscapes are significantly larger compared with those for the corresponding original fractals. The scale-free behaviors are non-trivial properties resulting from the fractal patterns.

It should be noted that in a considerably wide range of scale, a power-law function cannot be distinguished from an exponential one if β is large (e.g., $\beta \geq 3.0$). In the present paper, we fit the degree distributions of the RCVGs for the shuffled landscapes with a power-law function.

For the special case of $p = 0.25$, we have $p_{11} = p_{12} = p_{21} = p_{22} = 0.25$, which generates a trivial landscape with all the probabilities in the cells the same. For this extreme case, the degree distribution function is $\delta(k-4)$. A slight deviation of p from this special value may lead a deformation of the degree distribution function from the perfect δ function to a sharp peak, which can be regarded in a certain degree as a scale-free function with a large β. Hence, β reaches the maximum near the point $p = 0.25$.

The increase step of p is selected to be 0.045 to avoid the trivial value of $p = 0.25$. From the curves in Figs. 3 and 4, we can find that the more homogeneous a landscape, the larger value of β and the smaller values of $\langle C \rangle$ and $\langle R_{\text{cluster}} \rangle$. The curves are asymmetric with respect to the point of $p = 0.25$. To understand the asymmetrical behavior, let us consider two cases, $p = 0.25 - \xi$ and $p = 0.25 + \xi$, where ξ is a small deviation. The corresponding seeds are $[0.25-\xi, 0.25+(\xi/3), 0.25+(\xi/3), 0.25+(\xi/3)]$ and $[0.25+\xi, 0.25-(\xi/3), 0.25-(\xi/3), 0.25-(\xi/3)]$. Because $[0.25+(\xi/3)]/(0.25-\xi) > (0.25+\xi)/[0.25-(\xi/3)]$, the second case is comparatively more homogeneous than the first one. Hence, the right parts of the curves are much more homogeneous and consequently the maximum value of β and the minimum values of $\langle C \rangle$ and $\langle R_{\text{cluster}} \rangle$ occur at $p = 0.27$.

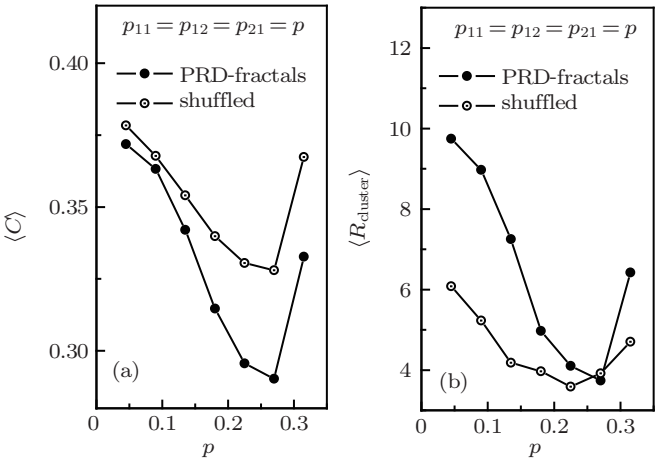


Fig. 4. (color online) Average clustering coefficient $\langle C \rangle$ and average cluster coverage $\langle R_{\text{cluster}} \rangle$ versus p. (a) The $\langle C \rangle$ for the PRD-fractals are smaller than for the corresponding shuffled landscapes, however, the difference becomes significant only when p is near 0.25. (b) With the increase of p, $\langle R_{\text{cluster}} \rangle$ decreases and reaches the minima at $p = 0.25$, and then increases. When p deviates significantly from the point $p = 0.25$, there exist distinguished differences between the original and the shuffled landscapes.

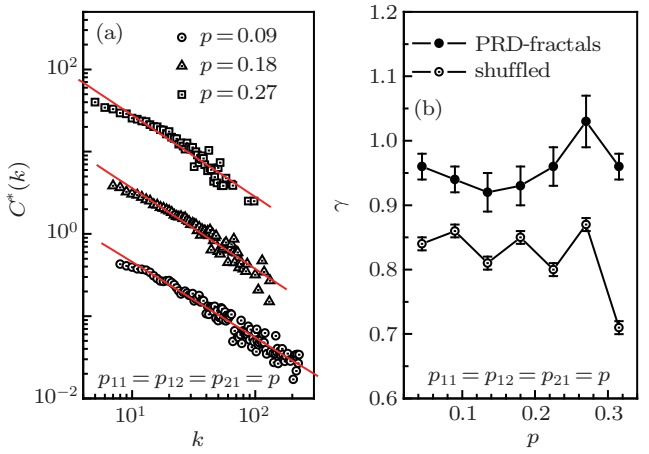


Fig. 5. (color online) Hierarchical structures of RCVGs for PRD-fractals. The generator is $(p_{11}, p_{12}, p_{21}, p_{22}) = (p, p, p, 1-3p)$. (a) The $C^*(k)$ versus k obeys a power law. The curves are vertically shifted for visualization convenience. (b) The γ for the shuffled landscapes are significantly smaller compared with that for the corresponding original fractals. The hierarchical behaviors are non-trivial properties resulting from the fractal patterns.

Figure 5 presents the hierarchical behaviors of the RCVGs for PRD-fractals. The RCVGs for the original landscapes have almost perfect hierarchical structures, i.e., the $C^{\star}(k)$ versus k obeys almost a power law perfectly, as shown in Fig. 5(a), and the values of $\gamma \geq 0.92$ are very close to 1 (Fig. 5(b)). What is more, γ of the RCVGs for the original landscapes are significantly larger than that for the corresponding shuffled landscapes (~ 0.84, almost the same with that for

the normally distributed landscapes in Fig. 2). That is, the hierarchical structures come from the nontrivial patterns in the PRD-fractals.

An interesting problem is the relation between the fractal and the topological properties. Figure 6 presents β versus H. The PRD-fractals are generated with randomly selected seeds without any other constraints on the generator P_0 except $p_{11}+p_{12}+p_{21}+p_{22}=1$. In total, 50 cases are produced. Though there roughly exists a negative correlation between β and H, the deviations of β from the linear regression are unacceptably large and are significantly larger compared with the errors. Hence, the topological properties can present new information on the landscapes.

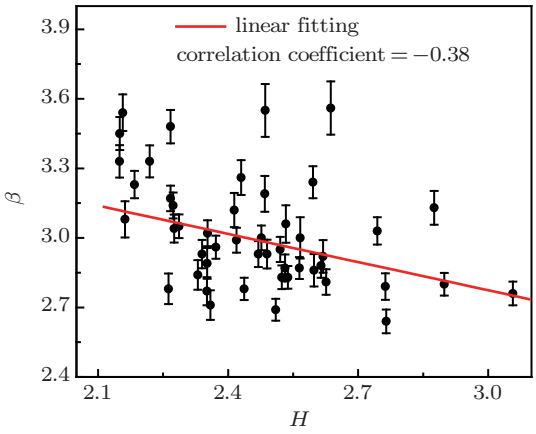


Fig. 6. (color online) Correlation between topological and scaling properties, namely, β versus H for PRD-fractals. The generators are chosen randomly without any constraints on the elements of P_0. There exists a negative correlation, however, the deviations of β from the linear regression are significantly larger compared with the errors.

For the MDA-fractals, the degree distributions decay exponentially, as shown in Fig. 7. The α for the shuffled landscapes are significantly larger than that for the corresponding original fractals. The exponential behaviors are non-trivial properties resulting from the fractal patterns. When H is large enough ($H > 0.3$ in the curve), with the increase of H, α for the original landscape decreases rapidly, while that for the shuffled landscape increases slowly, which leads to the increasing difference between them. This can be understood by the persistence of the MDA-fractals. A large value of H means a persistent behavior of a MDA-fractal, which means a high probability of a node being connected with other nodes. The shuffling procedure tends to cut-off the long-range edges existing in the RCVG for the original landscape.

Figure 8 shows average clustering coefficient $\langle C\rangle$ and average cluster coverage $\langle R_{\rm cluster}\rangle$ versus H. The $\langle C\rangle$ for the MDA-fractals are larger than that for the corresponding shuffled landscapes, however, there are no significant differences between them. When $H \le 0.5$, there are no significant differences between $\langle R_{\rm cluster}\rangle$ for the original and the shuffled landscapes, while in the interval of $0.5 > H > 0.9$, there appears a peak with significantly large $\langle R_{\rm cluster}\rangle$ for the original MDA-fractals. When H is small, the added errors, w, in Eq. (11) are large and determine the behaviors of the generated landscapes. When H becomes larger than 0.5, the increase of persistence induces a significant extension of the clusters. However, when H becomes very close to 1, the added errors vanish and the behaviors of the MDA-fractals are determined by the special procedure of the algorithm. This is why the peak appears.

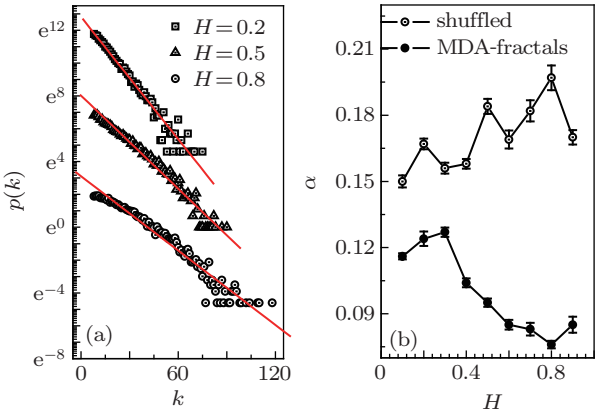


Fig. 7. (color online) Degree distributions of RCVGs for MDA-fractals. (a) The degree distribution functions obey an exponential law. The curves are vertically shifted for visualization convenience. The average degrees for $H = 0.2$, 0.5, 0.8 are $\sim$ 13, 17, 21, respectively. (b) The α for the shuffled landscapes are significantly larger compared with that for the corresponding original fractals. When H is large enough ($H > 0.3$ in the curve), with the increase of H, α for the original landscape decreases rapidly, while that for the shuffled landscapes increases slowly, which leads to the increasing difference between them.

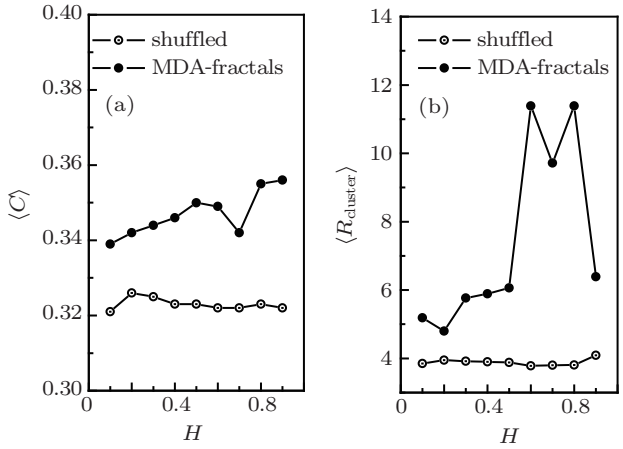


Fig. 8. (color online) Average clustering coefficient $\langle C\rangle$ and average cluster coverage $\langle R_{\rm cluster}\rangle$ versus H. (a) The $\langle C\rangle$ for the MDA-fractals are larger than that for the corresponding shuffled landscapes, however, there is no significant difference between them. (b) When $H \le 0.5$, there is no significant difference between $\langle R_{\rm cluster}\rangle$ for the original and the shuffled landscapes, while in the interval of $0.5 > H > 0.9$, there appears a peak with significantly large $\langle R_{\rm cluster}\rangle$ for the original MDA-fractals.

Figure 9 presents the hierarchical behaviors of RCVGs for MDA-fractals. The $C^*(k)$ versus k obeys a power law, as shown Fig. 9(a). In the interval of $H < 0.5$, γ for the original and the shuffled landscapes are almost the same and the

RCVGs have almost perfect hierarchical structures. When $H \geq 0.5$, with the increase of persistence in the original landscape, γ decreases rapidly from 0.74 (at $H = 0.5$) to 0.34 (at $H = 0.9$), i.e., the hierarchical structures are destroyed completely.

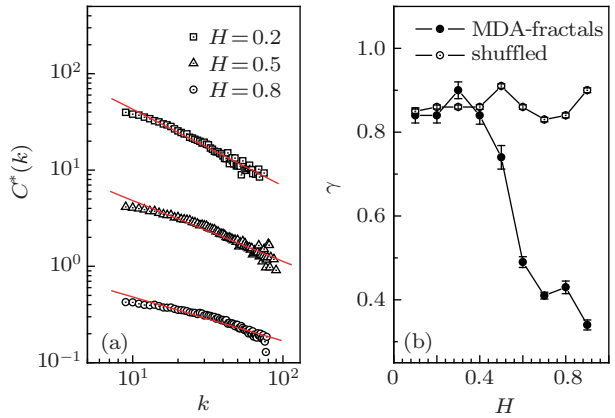


Fig. 9. (color online) Hierarchical structures of RCVGs for MDA-fractals. (a) The $C^*(k)$ versus k obeys a power-law. (b) In the interval of $H < 0.5$, γ for the original and shuffled landscapes are almost the same. When $H \geq 0.5$, with the increase of H, γ decreases rapidly from 0.74 (at $H = 0.5$) to 0.34 (at $H = 0.9$).

4. Conclusions

The network-based approach to 1D landscapes has made great progress in recent years.[38,40,56–59] In the present paper, we propose a simplified version of the standard visibility graph, called RCVG, to capture the characteristics of two-dimensional landscapes.

The RCVGs for PRD-fractals behave scale-free. They have pattern-induced hierarchical organizations and comparatively much more extensive structures. The scale-free exponent has a negative correlation with the Hurst exponent, however, there is no deterministic relation between them, i.e., the RCVG can detect new information rather than the wavelet analysis.

The RCVGS for the MDA-fractals are exponential networks. When the Hurst exponent is large enough (e.g., $H > 0.5$), the degree distribution decays much more slowly, the average coverage becomes significantly large and the initially hierarchical structure at $H < 0.5$ is destroyed completely.

Landscapes generated with different mechanisms behave differently qualitatively, while that generated with the same mechanism but different parameters behave differently quantitatively. The visibility graph can detect the difference of PRD- and MDA-fractals, which cannot be displayed by using the fractal spectrum in the wavelet analysis. What is more, each node and local pattern in the visibility graph has a perfect coordinate in the Euclidean space, namely, the network is embedded in the Euclidean space. We can consider the topological and the Euclidean properties simultaneously. This is one of the advantages of the visibility graph, comparing with other tools such as the wavelet analysis. Hence, the RCVG can be used to detect the pattern-related new characteristics of two-dimensional landscapes.

Because of the restriction of searching only the row- and the column–visibility relationships, the generalization of the RCVG to high-dimensional systems is straight-forward. As an example, for a three-dimensional (3D) system, we can construct a network by linking each node with all the nodes in the row, the column, and the height that are within its visible line. The network can capture the nontrivial patterns in the 3D structure. It may be useful in capturing the structural characteristics of pore media and so on.

At the same time, the restriction is feasible even in the case of real-world complex surfaces where distinct directions (coordinates) do not necessarily exist. The "direction" restriction should be understood as the features (independent of each other) that we are interested in, rather than the directions in the Euclidean space. For example, let us consider the evolutionary process of a system whose units distribute in the Euclidean space, the network will be a row–column–time visibility graph. For a surface on a global system, the simple relaxation of the restriction is to construct a longitude–latitude visibility graph. For each node, the elements on the longitude and the latitude it sits on are regarded as two time series, respectively. For each time series, we can use the one-dimensional visibility graph algorithm. Hence, the restriction can be relaxed easily in many real-world complex surfaces.

It should be noted that the RCVG is not a trivial use of two one-dimensional visibility graphs. Firstly, one-dimensional MDA-fractals are widely used to simulate fractional Brownian motions, the visibility graphs of which behave scale-free, as proved in Ref. [39]. A straight-forward deduction is that the visibility graphs for the rows and the columns of a two-dimensional MDA-fractal should behave scale-free, because the rows and the columns are the sections (boundaries) of the MDA-fractal. However, the RCVGs for two-dimensional MDA-fractals turn out to be exponential networks, which should be a result of the couplings between rows and columns. Secondly, the concept of RCVG can be used to deal with the evolutionary process for a system whose elements distribute in real-world space. Thirdly, a comparison of the results for the two kinds of fractals tells us that the method in the present work can provide us with new interesting information that is different from the methods in the literature, such as the wavelet analysis. By means of the traditional series analysis, one cannot distinguish between the two kinds of time series, while by means of the visibility graph, the differences are displayed explicitly. Further application of the visibility graph is to detect the structural patterns from micro- to macro-scales.

In the present work, we consider several kinds of landscapes generated by theoretical models. Actually, in the litera-

ture, investigations on the visibility graph focus mainly on the time series generated by perfect models rather than real world data. Once we try to deal with real-world landscapes, we must consider the effects of noise, a mixture of different kinds of landscapes, trends, finite sizes of records, etc. We have done some work on the mixture problem for a one-dimensional visibility graph.[70] To understand the results for real-world landscapes, detailed and systematic works based upon model-generated landscapes are required to serve as benchmarks.

References

[1] Anfinsen C B 1973 *Science* **181** 223
[2] Baldwin R L and Rose G D 1999 *Trends Biochem. Sci.* **24** 26
[3] Anderson P W 1958 *Phys. Rev.* **109** 1492
[4] Lee P A and Ramakrishnan T V 1958 *Rev. Mod. Phys.* **57** 287
[5] Kohmoto M, Sutherland B and Tang C 1987 *Phys. Rev. B* **35** 1020
[6] Albuquerque E L and Cottam M G 2003 *Phys. Rep.* **376** 225
[7] Yang H, Zhao F, Qi L and Hu B 2004 *Phys. Rev. E* **69** 066104
[8] Zhao F, Yang H and Wang B 2005 *Phys. Rev. E* **72** 046119
[9] Yang H, Zhao F and Wang B 2006 *Physica A* **364** 544
[10] Yang H, Zhao F and Wang B 2006 *Chaos* **16** 043112
[11] Yang H, Zhu G, Yin C and Li B 2008 *Phys. Rev. E* **77** 045101
[12] Zhu G, Yang H, Yin C and Li B 2008 *Phys. Rev. E* **77** 066113
[13] Einstein A 1905 *Ann Physics* **17** 549
[14] Metzler R and Klafter J 2000 *Phys. Rep.* **339** 1
[15] Sokolov I M and Klafter J 2005 *Chaos* **15** 026103
[16] Klafter J and Sokolov I M 2005 *Phys. World* **18** 29
[17] Brockmann D, Hufnagel L and Geisel T 2006 *Nature* **439** 462
[18] Klages R, Radons G and Sokolov I M 2008 *Anomalous Transport: Foundations and Applications* (Weinheim: VCH Wiley)
[19] Scher H and Montroll E W 1975 *Phys. Rev. B* **12** 2455
[20] Wong I Y, Gardel M L, Reichmann D R, Weeks E R, Valentine M T, Bausch A R and Weitz D A 2004 *Phys. Rev. Lett.* **92** 178101
[21] Dentz M, Cortis A, Scher H and Berkowitz B 2004 *Adv. Water Resources* **27** 155
[22] Kosztolowicz T, Dworecki K and Mrowczynski S 2005 *Phys. Rev. Lett.* **94** 170602
[23] Banks D S and Fradin C 2005 *Biophys. J.* **89** 2960
[24] Golding I and Cox E C 2006 *Phys. Rev. Lett.* **96** 098102
[25] Zimmermann W, Sesselberg M and Petruccione F 1993 *Phys. Rev. E* **48** 2699
[26] Zimmermann W, Painter B and Behringer R 1998 *Eur. Phys. J. B* **5** 575
[27] Sokolov I M, Schmidt G W and Sagues F 2006 *Phys. Rev. E* **73** 031102
[28] Alonso S, Kapral R and M. Bär 2009 *Phys. Rev. Lett.* **102** 238302
[29] Viscek T, Ben-Jacob E, Cohen I and Shochet O 1995 *Phys. Rev. Lett.* **75** 1226
[30] Schweitzer F, Tilch B and Ebeling W 1998 *Phys. Rev. Lett.* **80** 5044
[31] Dan D and Jayannavar A M 2002 *Phys. Rev. E* **66** 041106
[32] Dunkel J and Hänggi P 2005 *Phys. Rev. E* **71** 016124
[33] Lindner B 2007 *New J. Phys.* **9** 136
[34] Burgis M, Schaller V, Glässl M, Kaiser B, Köhler W, Krekhov A and Zimmermann W 2010 arXiv:1010.3115v1[cond-mat.stat-mech]
[35] Ivanov P CH, Amaral L A N, Goldberger A L, Havlin S, Rosenblum M G, Struzik Z R and Stanley H E 1999 *Nature* **399** 461
[36] Li B and Wu Z 1993 *Phys. Rev. B* **47** 3638
[37] http://en.wikipedia.org/wiki/Visibility_graph
[38] Lacasa L, Luque B, Bllesteros F, Luque J and Nuno J C 2008 *Proc. Natl. Acad. Sci. USA* **105** 4972
[39] Lacasa L, Luque B, Luque J and Nuno J C 2009 *Europhys. Lett.* **86** 30001
[40] Ni X, Jiang Z and Zhou W 2009 *Phys. Lett. A* **373** 3822
[41] Luque B, Lacasa L, Ballesteros F and Luque J 2009 *Phys. Rev. E* **80** 046103
[42] Yang Y, Wang J, Yang H and Mang J 2009 *Physica A* **388** 4431
[43] Shao Z 2010 *Appl. Phys. Lett.* **96** 073703
[44] Zhao D and Li X 2010 *Appl. Phys. Lett.* **96** 266101
[45] Albert R and Barabasi A L 2002 *Rev. Mod. Phys.* **74** 47
[46] Newman M E J 2005 *Contemp. Phys.* **46** 323
[47] Clauset A, Shalizi C R and Newman M E J 2009 *SIAM Review* **51** 661
[48] Barabasi A L, Ravasz E and Vicsek T 2001 *Physica A* **299** 559
[49] Dorogovtsev S N, Goltsev A V and Mendes J F F 2002 *Phys. Rev. E* **65** 066122
[50] Jung S, Kim S and Kahng B 2002 *Phys. Rev. E* **65** 056101
[51] Vazquez A, Pastor-Satorras R and Vespignani A 2002 *Phys. Rev. E* **65** 066130
[52] Ravasz E, Somera A L, Mongru D A, Oltvai Z N and Barabasi A L 2002 *Science* **297** 1551
[53] Vazquez A 2003 *Phys. Rev. E* **67** 056104
[54] Sun X and Wu Z 2001 *Acta Phys. Sin.* **50** 2126 (in Chinese)
[55] Fournier A, Fussel D and Carpenter L 1982 *Communications of the ACM* **25** 371
[56] Zhang J and Small M 2006 *Phys. Rev. Lett.* **96** 238701
[57] Zhang J, Luo X, Nakamura T, Sun J and Small M 2007 *Phys. Rev. E* **75** 016218
[58] Xu X, Zhang J and Small M 2008 *Proc. Natl. Acad. Sci. USA* **105** 19601
[59] Zhang J, Sun J, Luo X, Zhang K, Nakamura T and Small M 2008 *Physica D* **237** 2856
[60] Yang Y and Yang H 2008 *Physica A* **387** 1381
[61] Hirata Y, Horai S and Aihara K 2008 *Eur. Phys. J. Spec. Top.* **164** 13
[62] Haraguchi Y, Shimada Y, Ikeguchi T and Aihara K 2009 *ICANN 2009, Part II, LNCS* **5769** 325
[63] Wang J and Yang H 2009 *Mod. Phys. Lett. B* **23** 1781
[64] Marwan N, Donges J F, Zou Y, Donner R V and Kurths J 2009 *Phys. Lett. A* **373** 4246
[65] Donner R V, Small M, Donges J F, Marwan N, Zou Y, Xiang R and Kurths J 2011 *Int. J. Bifurcation Chaos* **21** 1019
[66] Donner R V, Zou Y, Donges J F, Marwan N and Kurths J 2010 *Phys. Rev. E* **81** 015101
[67] Donner R V, Zou Y, Donges J F, Marwan N and Kurths J 2010 *New J. Phys.* **12** 033025
[68] Sinatra R, Condorelli D and Latora V 2010 *Phys. Rev. Lett.* **105** 178702
[69] Xie W and Zhou W 2011 *Physica A* **390** 3592
[70] Qi J, Wang J, Wang J, Xiao Q and Yang H 2011 *Fluctuation and Noise Letters* **10** 371